*Plasma Physics Reports, Vol. 31, No. 4, 2005, pp. 314–324. Translated from Fizika Plazmy, Vol. 31, No. 3, 2005, pp. 350–360.*


**SPACE PLASMA**

# Manifestation of Quasilinear Diffusion on Whistlers in the Fine-Structure Radio Sources of Solar Radio Bursts

**G. P. Chernov**

*Institute of Terrestrial Magnetism, Ionosphere, and Radio-Wave Propagation, Russian Academy of Sciences, Troitsk, Moscow oblast, 142092 Russia*

Received November 17, 2004

**Abstract**—The zebra structure and fiber bursts in the dynamic spectra of the solar type IV radio burst recorded on October 25, 1994, are analyzed using observational data from ground-based stations and Earth-orbiting satellites. The fine structure is observed when new hot magnetic loops, in which high- and low-frequency plasma instabilities develop, ascend to the solar corona. The frequency range of the fine structure is determined by the dimensions of these loops. The main features of the zebra structure are analyzed in terms of the interaction of plasma waves with whistlers. The results obtained are compared to the predictions from the double plasma resonance model. © *2005 Pleiades Publishing, Inc.*

## 1. INTRODUCTION

The emission and absorption stripes against the continuum background of the solar type IV radio bursts are conventionally divided into two groups: the so-called zebra-structure (ZS) and fiber bursts. The ZS consists of more or less regular stripes in the dynamic spectrum with a generally positive but time-varying frequency drift. The fiber bursts are usually characterized by a nearly constant negative frequency drift. These structures have long been studied, and their properties are well known (see, e.g., [1, 2]). In some cases, however, unusual stripes with rapidly varying parameters have been observed. Similar features of the fine structure in the microwave range have recently been revealed with the novel spectrograph of the Peking observatory [3, 4]. The measurements were performed in the 2.6- to 3.8-GHz frequency range (each 8 ms) with a frequency resolution of 10 MHz.

The interpretation of such a complicated fine structure has always lagged behind the acquisition of new observational data. As for fiber bursts, however, it is now commonly accepted that they are emitted due to the interaction of electrostatic plasma waves ($l$) with whistlers ($w$) that are excited by the same fast electrons with a loss-cone velocity distribution. This interaction gives rise to an ordinary wave ($t$), which then freely escapes from the plasma: $l + w \longrightarrow t$ [5].

Mechanisms for the formation of the zebra structure are still not quite clear. More than ten different models have been proposed, most of which involve the conversion of electrostatic plasma waves at the double plasma resonance [5–10]:

$$\omega_{UH} = (\omega_{Pe}^2 + \omega_{Be}^2)^{1/2} = s\omega_{Be}, \qquad (1)$$

where $\omega_{UH}$ is the upper hybrid frequency, $\omega_{Pe}$ is the electron plasma frequency, $\omega_{Be}$ is the electron cyclotron frequency, and $s$ is the harmonic number. The model proposed in [10] is most adequate to observations and the corona conditions; it is based on the unsaturated electron-cyclotron maser emission from electrons with a loss-cone velocity distribution. However, all similar theories of the zebra structure encounter the following difficulties:

(i) The frequency separation $\Delta f_s$ between the stripes of the ZS should be equal to a certain fraction of the electron cyclotron frequency (depending on the relation between the height scales of the magnetic field and density in the corona). However, irregular structures are frequently observed.

(ii) The magnetic field determined from the $\Delta f_s$ value is always too low for the obvious inequality $\beta \approx (v_s/v_A)^2 \ll 1$ to be satisfied in the magnetic trap above the active region (AR) (here, $v_s$ and $v_A$ are the ion acoustic and the Alfvén velocities, respectively).

(iii) Almost all the models account only for the emission stripes, although the absorption stripes sometimes dominate.

(iv) All the models ignore an important property of the loss-cone velocity distribution: the generation of whistlers. The interaction of whistlers with fast particles drastically changes the velocity distribution: the transverse anisotropy decreases and a longitudinal particle beam arises.

The fact that the main spectral features of the ZS stripes and fibers, as well as their polarization, are the same indicates that the emission mechanism is also the same for both structures and is associated with the coupling of plasma waves with whistlers, although under different conditions of whistler excitation. The magnetic trap is entirely occupied by periodic wave

1063-780X/05/3104-0314$26.00 

packets of whistlers that are excited at the cyclotron resonance,

$$\omega_w - k_\parallel v_\parallel - s\omega_{Be} = 0, \quad (2)$$

by fast electrons with a loss-cone distribution. Here, $\omega_w$ is the whistler frequency, $k_\parallel$ is the whistler longitudinal wavenumber, and $v_\parallel$ is the longitudinal velocity of the fast electrons.

Depending on the shape of the distribution function, the instability develops under conditions corresponding either to the normal Doppler resonance ($s = +1$), at which whistlers and fast particles propagate in opposite directions along the magnetic field, or to the anomalous resonance ($s = -1$), at which the whistlers and the fast particles propagate in the same direction at a large angle to the magnetic field. In the former case, fiber bursts are generated, whereas in the latter case, ZSs with different frequency drifts form [11–15]. The fast periodicity of the whistler instability is primarily related to its quasilinear behavior (the scattering of whistler by fast particles), which leads to periodic disruptions of the instability of electrostatic waves in the whistler packet. As a result, absorption stripes arise in both fiber bursts and ZSs [16]. Whistlers may also contribute to the emission and absorption stripes due to their interaction with plasma waves at both the sum and difference frequencies, $\omega_l \pm \omega_w = \omega_t$ [17–19].

The lack of a universal ZS theory has stimulated the development of new models involving the interaction at the double plasma resonance. In [20], the magnetic field in the corona was supposed to decrease with height much more rapidly than the density. Attributing the observed emission to the second harmonic of $\omega_{UH}$, the authors of [20] obtained more realistic values of the magnetic field as compared to the those obtained in [3] within the whistler model. However, ZSs are usually highly polarized (moderate polarization is very seldom), which precludes the generation at the second harmonic. As a result, in [20], the magnetic field $B$ was overestimated by a factor more than 2; moreover, the harmonic number $s$ was chosen arbitrarily.

To avoid difficulties related to too low values of the magnetic field at the double plasma resonance, a new theory of ZSs was proposed in [21]. The theory is based on the emission of the so-called auroral choruses recorded by ground-based stations. These are magnetospheric bursts at frequencies of 2–4 MHz with a fine structure similar to ZSs. It is assumed (by analogy with [10]) that these bursts are related to the generation of the $Z$ mode at the upper hybrid frequency via the cyclotron maser mechanism. Although the $Z$ mode itself does not escape from the source, it can transform into ordinary (O) modes at discrete frequencies (eigenmodes) in the presence of density inhomogeneities. The problem thus reduces to solving the Shrödinger equation for the $Z$ mode captured by a cylindrical density inhomogeneity in the Wentzel–Kramers–Brillouin approximation. The eigenmodes arise due to quantization under the eikonal conditions when waves with proper azimuthal ($m$) and radial ($n$) quantum numbers escape through the co-called Ellis windows. The $Z$ modes can be generated by a point source at a given harmonic number of the double plasma resonance ($s = 2$ in Eq. (1)). The main distinctive feature and advantage of this model are that it allows for the generation of a large number (up to 100) of harmonics with a small frequency separation, $\Delta f_s \approx 0.01 f_{Be}$. The required amplitude of the density variations and the size of inhomogeneities were estimated in [21] at <10% and 1–100 m, respectively. Such inhomogeneities can be produced by dispersive ion-acoustic waves. However, in [21], a very important issue—the time dependence of the eigenmodes (the ZS dynamics)—was not considered and only the possible stability of inhomogeneities over a time interval of ~10 s was discussed. Conditions for the excitation of ion-acoustic waves, including the main requirement that the electron temperature should be much higher than the ion temperature, $T_e \gg T_i$, which is satisfied in the solar corona only in turbulent plasma with anomalous resistance (e.g., in current sheets and at shock fronts [22]), also were not analyzed. Moreover, the overall picture arising from many inhomogeneities produced by propagating ion–acoustic waves should spread the stripes into a continuous spectrum (continuum). The origin of fibers against the ZS background also was not considered. The other discrepancies between theory and observations will be discussed in Section 4.

Observations of the fine structure of the solar radio emission remain a reliable means for both diagnosing the solar corona and verifying the results of laboratory plasma experiments on the wave–wave and wave–particle interactions.

In recent years, observations of the fine structure of the solar radio emission have been substantially expanded and new properties of ZSs have been revealed. At present, an analysis of new effects implies a more thorough study of the burst processes in the optical and X-ray spectral ranges. Therefore, it is important to find out new features of the fine structure and to analyze them using different theoretical models. The present paper is devoted to studying this problem using the ZS in the solar radio burst recorder on October 25, 1994, as an example. Some features of this burst were previously analyzed in [23–25]; the main unusual properties of the ZS were not considered, however.

## 2. OBSERVATIONS

ZSs were analyzed using the 1994 10 25 event in the meter wavelength range as an example. We used the data from simultaneous observations with several radio spectrographs: the 100- to 500-MHz ARTEMIS spectrograph at the Nançay observatory; the 25- to 270-MHz spectrograph at the Institute of Terrestrial Magnetism, Ionosphere, and Radio-Wave Propagation of the

Russian Academy of Sciences (IZMIRAN, Troitsk); and the 400- to 800-MHz spectrograph at the Tremsdorf observatory (Potsdam), as well as the data from the Nançay radioheliograph (NRH) and the Triest polarimeter at frequencies of 237, 327, and 408 MHz. The radio event consisted of a type II burst drifting from frequencies below 90 MHz at 10:00 UT to 40 MHz at 10:06 UT, a short type IV burst (burst continuum) with a fine structure in the form of periodic type III bursts between 10:05:18 and 10:08:35 UT, and a ZS between 10:08:00 and 10:09:00 UT.

The dynamic spectrum observed with the ARTEMIS spectrograph is shown in Fig. 1a. The type III bursts drift very rapidly over frequency (perhaps, due to the elevated plasma density above the burst region). At lower frequencies, however, the drift is much slower. The emission energy was mainly concentrated in the meter wavelength range. The maximal spectral intensity at a frequency of 204 MHz was 300–400 sfu[1] between 10:08 and 10:09 UT. A minor (49 sfu) GRF-type microwave burst was observed over about one hour. According to *Solar Geophysical Data, No. 608 (II), 1994*, a small $H_\alpha$ flare of 1N importance was observed from 09:40 to 12:36 UT (with a maximum at 10:04 UT) in the 7792 (S09, W12) AR. An active dark filament and a filament system over this AR were also observed. Some details of this type IV radio burst with different locations of the radio source beyond the AR were discussed in [23].

Figure 1b shows the spatial distribution of the radio emission intensity superimposed on the soft X-ray (SXR) burst image (Yohkoh/SXT) recorded using a 1-μm Al filter. It can be seen that the center of the radio source of the fine structure at 164 MHz (NRH) is located beyond the AR. However, the source of the main continuum coincides with the maximum of the SXR burst. Each subsequent SXR image shows new bright sources both inside and beyond the main burst region; this points to the magnetic reconnection of the flare loop with neighboring loops. Probably, it is for this reason that repetitive bursts of radio emission at 327 and 408 MHz (Triest observatory) had different polarizations. The maxima of the SXR brightness occurred at the same place (in the center of the AR over the neutral line) at 09:59 UT (before the type II burst) and at 10:08 UT (during the type III burst). Sigmoid shape of the SXR burst followed the shape of the neutral line of the magnetic field. It was supposed in [24] that the flare triggered a large-scale magnetic reconnection.

In this event, the ZS was observed in the frequency range 130–210 MHz against the background of type III bursts drifting from 400 to 150–125 MHz (Fig. 1). Let us note the principal issues in Fig. 1 that elucidate the event dynamics. The initial frequency of type III bursts varied between 300 and 450 MHz with a period gradually increasing from 10–15 to 30–35 s during a series of type III bursts. This was possibly related to slow MHD oscillations of the region where the fast particles were accelerated. The lowest frequency of type III bursts varied asynchronously with their initial frequency and decreased to about 125 MHz between 10:08:12 and 10:08:30 UT.

An explicit indication of a new perturbation was that the frequency drift terminated abruptly between 10:07:38 and 10:07:57 UT at a frequency of 170 MHz (see Fig. 1c). About 3 s later, a ZS arose at frequencies of 140–170 MHz. By the end of the 8th min (10:08 UT), the ZS frequency range expanded to 130–210 MHz, whereas type III bursts gradually disappeared (their intensities and frequency bandwidths steadily decreased). In the time interval from 10:08:17 to 10:08:24 UT, within which the ZS was most pronounced, seventeen emission stripes with a frequency separation gradually increasing from 1.7 MHz at 140 MHz to about 2.2 MHz at 170 MHz were observed. The degree of polarization of radio emission in the ZS and type III bursts was rather moderate (25–30%) and reached its maximum in the ZS at the end of the 8th min. The sign of polarization of radio waves emitted from the source above the southern-polarity tail spot corresponded to the predominance of ordinary waves.

A part of the ZS dynamic spectrum recorded with the Potsdam spectrograph is shown in Fig. 2a. It is almost identical to the spectrum recorded at IZMIRAN. Figure 2b shows the contour lines of the south–north (SN) distribution of the radio emission intensity at a frequency of 164 MHz (NRH). The maximal intensity corresponds to the center of the ZS source after 10:08:33 UT or to a type III burst before this instant. The solid line that passes through the source centers shows the spatial drift of the sources at a fixed frequency. We note that the centers of the sources of the ZS and type III bursts coincide not only in the NS direction but also in the east–west (EW) direction (i.e., on the Sun disk). The III type sources (at the beginning of spectrum) drift from south to north, whereas the ZS sources (at the end of spectrum) drift from north to south. In all the ZS absorption stripes, the source drifts is the same way as in the type III bursts (one such instant corresponding to 10:08:33.4 UT is shown in Fig. 2 by the heavy vertical line). The labels on the vertical axis in Fig. 2b correspond to the numbers of the spatial channels of the Nançay radio interferometer. At a frequency of 164 MHz, one channel in the SN direction provides resolution of about 3.2' [26]. Therefore, the average full width at half-maximum of the radio source (about 4.8') corresponds to one-and-a-half channel for both the ZS and type III bursts, whereas the maximal velocity of the spatial drift turns out to be >90 000 km/s (about 170 000 km/s for the last source). Taking into account the projection onto the disk, the actual velocities of the source are always $>10^{10}$ cm/s (i.e., close to the speed of light). Thus, the measured source size is actually the AR size and the observed drift velocities can only be attributed to fast (relativis-

[1] One sfu (solar flux unit) is equal to $10^{-22}$ W/(m$^2$ Hz).

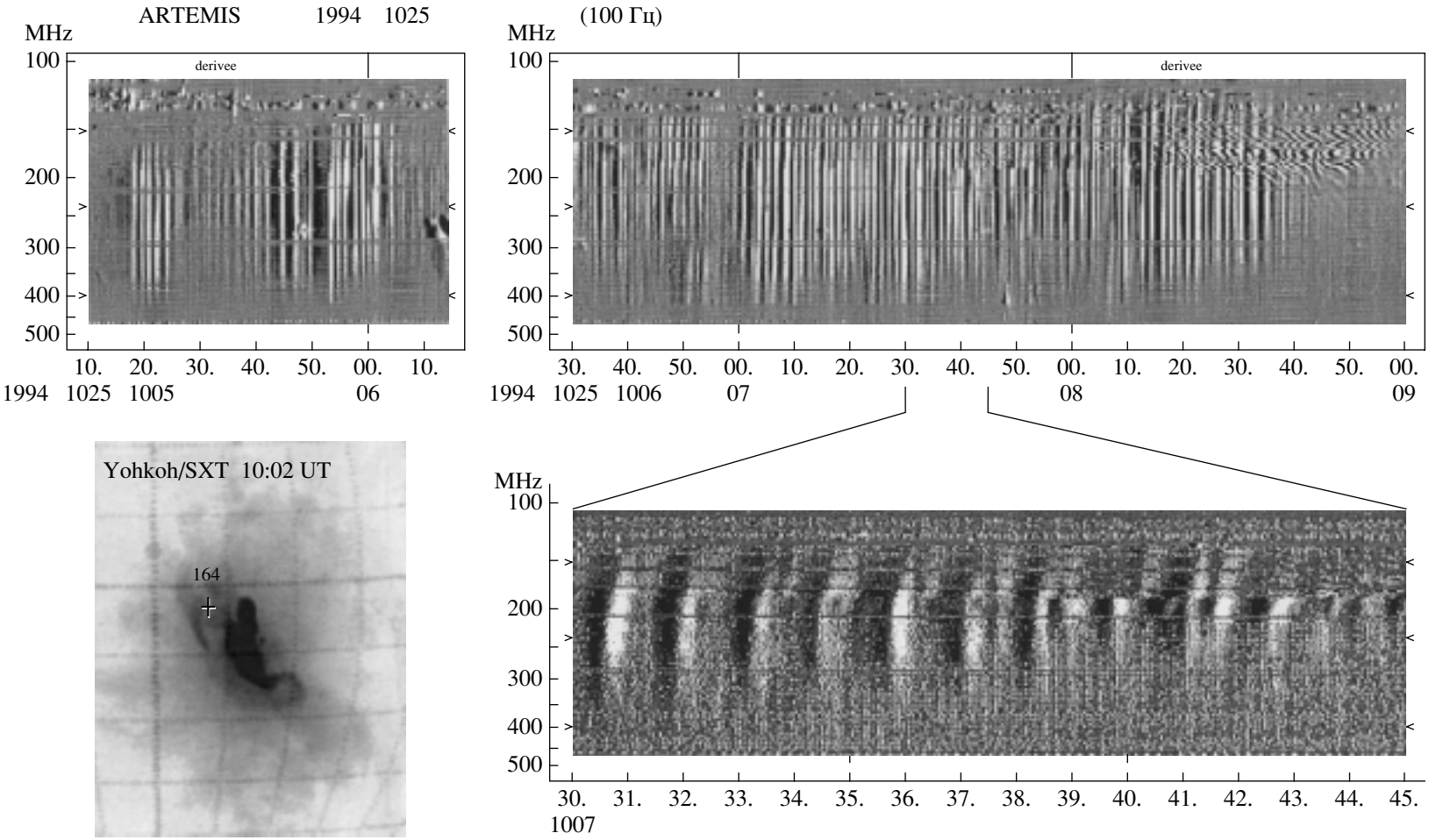


**Fig. 1.** (a) Dynamic spectrum (the derivative of the signal) of periodic type III bursts over the entire 100- to 500-MHz frequency range of the ARTEMIS spectrograph. It can be seen that a ZS appears in the frequency range of 135–210 MHz at the end of the event. In plot (c), a magnified fragment of the type III burst spectrum is shown, which demonstrates an abrupt stop of the frequency drift at a frequency of about 170 MHz. It can be seen in plot (b) that the center of the radio source at a frequency of 164 MHz (marked with a cross against a Yohkoh/SXT image) is located beyond the bright flare region.

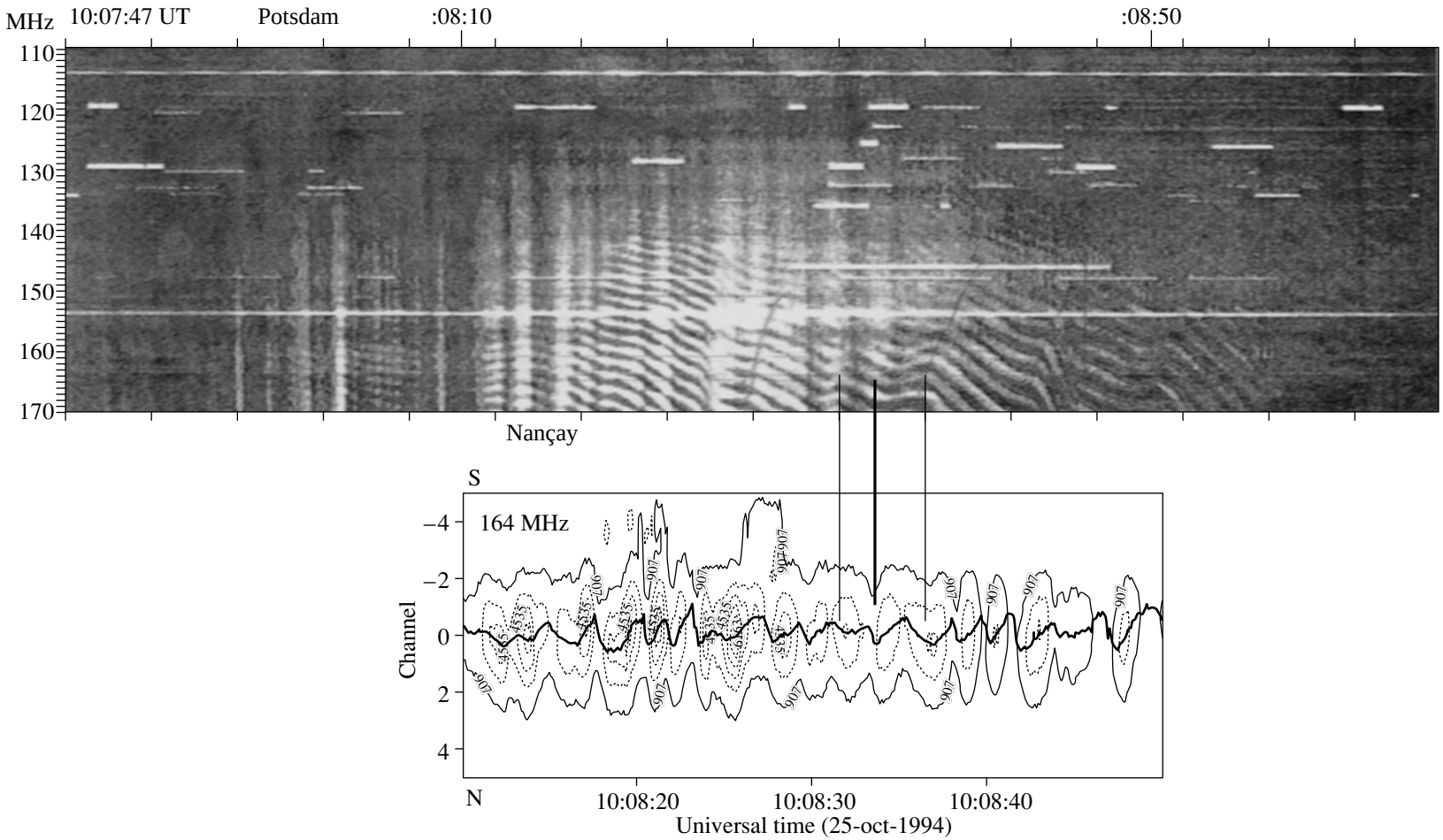


**Fig. 2.** (a) Dynamic spectrum of the ZS against the background of periodic type III bursts within the 100- to 170-MHz frequency range (a fraction of the data from the Potsdam spectrograph) and (b) the one-dimensional SN profile of the radio emission intensity measured with the NRH at a frequency of 164 MHz. The solid line passing through the centers of the sources in plot (b) shows their spatial drift.

tic) particles. Approximately the same drift velocities of the ZS sources were observed earlier during the 1990 06 05 event [26].

We also note the following important feature of the dynamic spectra: there are several humps in the ZS where the frequency drift changes its sign. The change in the sign of the frequency drift correlates with the change in the direction of the spatial drift of the ZS source. The negative frequency drift corresponds to the same source drift as for type III bursts. The change in the direction of the source drift is accompanied by the change in the sign of the frequency drift (see, e.g., the instants 10:08:32 and 10:08:36.5 UT in Fig. 2, which are marked by light vertical lines). These results allow one to explain the width of the frequency band occupied by the ZS in the dynamic spectrum (see Section 4). In the URAP experiment, the *Ulysses* satellite recorded one type III burst at 10:10 UT at frequencies below 1000 kHz. This burst was caused by an electron beam accelerated at the beginning of the burst.

## 3. GENERAL SCHEME FOR THE ORIGIN OF THE EMISSION AND ABSORPTION STRIPES IN THE WHISTLER MODEL

As was noted above, the generation of fiber bursts is commonly attributed to the merging of plasma waves with whistlers: $l + w \longrightarrow t$[5]. The ZS models usually involve the conversion of plasma waves at the double plasma resonance [5–10]. The most significant inconsistency of those models is that, on the one hand, in order to account for the dynamics of the ZS stripes, one has to assume that the magnetic field (or the background plasma density) varies rapidly over time and, on the other hand, the magnetic field determined from the frequency separation between the stripes is too low for the magnetic pressure to be much higher than the kinetic one ($\beta \ll 1$). Dark stripes in the ZS are actually related to the periodically modulated absorption of the background continuum, rather than merely to the lower intensity of the source. Recent KA TRACE observations showed that the burst loops in the 175- and 195-Å UV lines consist of numerous narrow loops, which do not expand upward and in which both the plasma density and the magnetic field vary only slightly with height. The occurrence of double plasma resonances in such loops is hardly possible.

The similarity between the main properties of the fiber bursts and the ZS stripes allows one to apply the whistler model to describing the ZS stripes. Type IV radio sources are generally regarded as magnetic traps; hence, it is natural to assume that the velocity distribution of the fast electrons responsible for continuum is a loss-cone Maxwellian distribution with an anisotropic temperature. Since such a distribution function is unstable against the excitation of whistlers, it is necessary to take into account variations in the distribution function due to the diffusion of the fast electrons on whistlers. Note that the excitation and propagation of whistlers in narrow burst loops is quite possible.

The conservation laws for the merging and decay processes with the participation of whistlers ($l + w \longrightarrow t$ and $l \longrightarrow t + w$) were considered in [27, 28] (as applied to the corona plasma, they were considered in [5, 19, 29]). Here, we will also assume that these laws are satisfied.

The formation of emission and absorption stripes is the main property of whistlers in type IV radio sources in the form of magnetic traps with a loss-cone distribution of the fast electrons [17]. Calculations of kinetic instabilities of whistlers [12] showed that the energy threshold for the excitation of whistlers is rather low. It was also shown that, in order to calculate the integral amplification coefficients of whistlers propagating at an arbitrary angle with respect to the magnetic field, one should take into account three main resonances: the Cherenkov resonance and the cyclotron resonances under conditions corresponding to the normal and anomalous Doppler effects.

An analysis of the quasilinear set of equations [30] showed that main feature of the linear whistler instability is its periodicity in both time and space. The time periodicity is very fast: the period is on the order of $10^{-3}$ s. Under the corona conditions, the diffusion time in a magnetic trap is usually much longer. Moreover, in this case, whistler instability should be modulated with the period of bounce oscillations (more exactly, with the period equal to the flight time of the fast particles between the top of the trap and the magnetic mirror, $l_B/(2v) \approx 0.5$ s, where $l_B$ is the trap length).

It was shown in [12] that, depending on the temperature anisotropy and the angle between the electron velocity and the magnetic field, the electron beam excites either whistlers propagating toward the beam (under conditions corresponding to the normal Doppler resonance: $v_\perp > v_\parallel$ and $s = 1$ in Eq. (2)) or those propagating along the beam at a large angle to the magnetic field (under conditions corresponding to the anomalous Doppler resonance: $v_\perp < v_\parallel$ and $s = -1$ in Eq. (2)).

The character of electron injection also plays an important role. For pulsed injection under conditions corresponding to the normal Doppler resonance (the particles and waves propagate away from one another in opposite directions), quasilinear effects do not operate. Under conditions corresponding to the anomalous resonance, the role of quasilinear effects increases with increasing injection duration (or if new particles come up with the wave).

In the case of whistler generation at the cyclotron resonances $s = \pm 1$, the fast resonant particles move along elliptic diffusion curves in the $(v_\perp, v_\parallel)$ plane down the gradient of the distribution function [31, 16]. Particles with small pitch angles transfer their energy to waves and approach the loss cone, whereas particles with large pitch angles gain energy from the waves ($v_\perp$

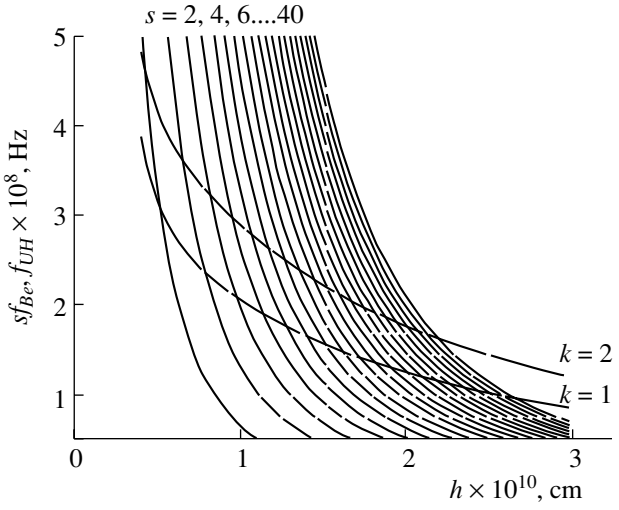


**Fig. 3.** Upper hybrid frequency $f_{UH}$ and electron gyrofrequency harmonics $sf_{Be}$ in the solar corona as functions of the height $h$ in the Newkirk model ($k$ = 1) and the double Newkirk model ($k$ = 2) of the electron density profile for a dipole magnetic field with $B$ = 2500 G at the photosphere level.

increases). However, only the particles immediately adjacent to the loss cone get into it; as a result, the loss cone remains almost empty over a long time. The estimated lifetime of the fast electrons scattered by whistlers in the regimes of moderate and strong diffusion is 10–20 s [32].

For a sufficiently long injection pulse, the generation of whistlers should be periodic in both time and space because the loss-cone instability is suppressed when the electrons fall into the loss cone and then (after 0.2–0.3 s) develops again when these electrons (and whistlers) leave the excitation region [5, 33]. It should be taken into account that particles can be scattered not only by whistlers but also by electrostatic waves [34, 35]. In this case, the electrons first diffuse on electrostatic waves toward lower $v_\parallel$ and then diffusion on whistlers along diffusion curves comes into play. The relaxation length of the beam exciting whistlers is [34]

$$l^w = \Lambda \frac{c}{\omega_{pe}} \frac{\omega_{Be}}{\omega_{pe}} \frac{n^c}{n^h}, \quad (3)$$

where $\Lambda \approx 25$ under the corona conditions. For $\omega_{pe}/2\pi = 1.5 \times 10^8$ Hz, $\omega_{pe}/\omega_{Be} = 30$, and a sufficiently low density of the fast (hot) electrons as compared to the density of the background cold plasma ($n^c/n^h \approx 3 \times 10^6$), we obtain $l^w \approx 0.8 \times 10^8$ cm. For the same parameters and an electron velocity of $v_\parallel \approx 1/3c$, the beam relaxation length on plasma waves is much larger: $l^l \approx 2.3 \times 10^9$ cm [16]. Thus, relaxation on whistlers is much faster, and the restriction on the initial angular spread of the beam, $\Delta\theta_0 > (l^w/l^l)^{1/3}$, at which relaxation on plasma waves can be ignored, is easily satisfied [34].

Over the time that is required for electrons to leave the loss cone ($T_c \approx l_B/(2v) \approx 0.25$ s for a trap length of $l_B \approx 5 \times 10^9$ cm), whistlers of frequency $\omega^w \approx 0.1\omega_{Be}$ propagating with the group velocity $v_{gr}^w \approx 5 \times 10^8$ cm/s cover a distance of $\Delta l_B = T_c v_{gr}^w \approx 1.25 \times 10^8$ cm [32]. Thus, due to the quasilinear relaxation of the beam on whistlers, all the trap will be divided into the zones of enhanced whistler excitation with a thicknesses $l^w$ and spatial period $\Delta l_B$. In this case, periodic packets of whistlers will produce regular ZS stripes with a frequency separation of $\Delta f_s \approx (l^w + \Delta l_B)|\nabla f_{pe}|$. In the double Newkirk model, we have $|\nabla f_{pe}| \approx 10^{-8}$ MHz/cm. Hence, for a frequency of 150 MHz, the frequency separation is $\Delta f_s \approx 2$ MHz, which coincides with that observed in the 1994 10 25 event.

The spectra of the generated whistlers are rather narrow [5]. The whistler group velocity is maximal at a frequency of $0.25f_{Be}$ and varies slightly at the spectrum wings (especially for obliquely propagating whistlers; see Fig. 5 in [17] and also [14] for details). This prevents whistler packets in the solar corona from spreading at the group velocity (as is the case for magnetospheric whistlers). Calculations of the possible whistler trajectories in the solar corona show that whistlers within the $\approx 0.05f_B$ band spread insignificantly over their propagation time ($\approx$10 s) [11]. Whistlers can be reflected from regions where their frequency approaches the lower hybrid (LH) frequency: $f^w \approx f_{LHR} \approx f_{Be}\sqrt{\frac{m_e}{m_p}}$. They can also be captured in regions with an increased plasma density (plasma ducts). Note that the spread in the whistler frequencies does not prevent this capture.

Thus, for a sufficiently long injection pulse, a fraction of the trap is occupied by periodic packets of whistlers (with a length $l^w$ along the trap). Each packet with a narrow spectrum forms a ZS stripe due to the merging with plasma waves. The propagation of a system of such packets at the group velocity gives rise to ZS stripes drifting to the levels of equal plasma density determined by the angles between the whistler trajectories and the magnetic field. A qualitative scheme of whistler trajectories was given in [13] (see Fig. 2c in that paper). Since the frequency ratio $f_{pe}/f_{Be}$ varies slightly within the height range of the ZS source, the group velocities of different packets are close in magnitude and direction even at the edges of this range. This prevents whistler packets from spreading and ensures a nearly synchronous frequency drift of the ZS stripes over the spectrum.

The positive frequency drift of the ZS stripes may be related to the excitation of obliquely propagating whistlers at the anomalous Doppler resonance at the top of the loop (where $v_\perp < v_\parallel$) and to the downward non-ducted propagation toward the LH resonance region,

from which the whistlers are reflected and then can again reach the top of the loop, where the instability growth rate is maximal. The downward propagation of whistlers toward the higher magnetic field prevents them from cyclotron damping because, in this case, $\omega^w/\omega_{Be}$ decreases. As a result, the ZS stripes persist over a longer time interval than the fiber bursts.

Fiber bursts with a dominant positive frequency drift are presumably related to the excitation of whistlers at the normal Doppler resonance near the trap base (i.e., near the magnetic mirror from which the particles are reflected and where the loss-cone angle is maximal). These longitudinal whistlers are ducted along the trap and then decay either due to cyclotron damping or (closer to the loop apex) because of the anomalous Doppler resonance.

The whistler model naturally accounts for the similarity between the main properties of fiber bursts and ZS stripes (the width, modulation depth, polarization, etc.). An occasionally observed continuous conversion of the fiber bursts into a ZS and vice versa can also be explained in terms of this model. As long as an unducted whistler propagates at a small angle with respect to $\nabla f_{pe}$ (i.e., almost along the trap), fiber bursts are observed. Near the top of the trap, the whistler may propagate along a curved trajectory that is nearly perpendicular to $\nabla f_{pe}$). In this case, the frequency drift slows down and the fiber bursts are transformed into ZS stripes, which sometimes keep staying nearly parallel to the time axis in the dynamic spectrum.

As the trap is filled with fast particles (during a long injection pulse), a self-oscillation regime of quasilinear diffusion on whistlers can be established. In this regime, instability switches between the normal and anomalous resonances (similarly to the fan instability [36] or the burst regime in tokamaks [37]). These switchings correspond to changes in the whistler propagation direction. This accounts for both regularly observed low-frequency undulatory variations in the rate of the frequency drift of the ZS stripes and abrupt jumps in the form of sawtooth stripes when the distribution function is perturbed by newly injected particles [16].

As was mentioned above, dark stripes in the ZS are actually related to the periodically modulated absorption of the background continuum, rather than merely to the lower intensity of the source. Absorption at the low-frequency edge of the emission stripe can be attributed to a decrease in the intensity of plasma waves (which are responsible for continuum) within a whistler packet due to the quasilinear diffusion of electrons on whistlers.

When whistlers are excited at the normal Doppler resonance due to the diffusion of fast particles on whistlers ($v_\perp > v_\parallel$), the maximum of the distribution function nearly instantaneously shifts toward larger longitudinal velocities (toward smaller pitch angles) and the instability of the plasma waves at the double plasma resonance is suppressed. This manifests itself in the form of dark ZS stripes. When diffusion on whistlers initially proceeds under conditions corresponding to the anomalous Doppler resonance ($v_\perp < v_\parallel$) and plasma waves propagating along the magnetic field are excited, their level also decreases due to the turn of the beam toward higher angles with respect to the magnetic field.

Unusual fiber bursts (without significant absorption) are sometimes observed in type II bursts. Such a fiber structure can be naturally related to the propagation of whistlers through plasma wave bunches ahead of a shock front. However, ahead of the shock front, there is no trap, particles and waves propagate independently of one another, and diffusion on whistlers does not come into play. As a result, plasma waves continue to be excited within whistler packets and absorption is absent.

Thus, taking into consideration quasilinear diffusion of fast electrons with a loss-cone velocity distribution on whistlers allows one to explain a number of important features of the fiber bursts and ZS.

## 4. DISCUSSION OF THE 1994 10 25 EVENT

In this short-term event, the ZS radio sources were located beyond the AR (see Fig. 1). A detailed analysis of Yohkoh/SXT images showed that an additional increase in the emission intensity outside the main flare region was caused by the magnetic reconnection of the main flare loop with the upper loops that previously existed in the corona.

The width of the ZS stripes is presumably determined by the distance between the X-point of magnetic reconnection above the flare loop and a point lying higher in the corona (in the shear region between the ascending flare loop and large transequatorial loops that are seen in Yohkoh/SXT images). An argument in favor of this assumption is that the low-frequency boundary of the ZS coincided with the frequency at which the drift of type III bursts terminated after 10:08:35 UT (see Fig. 1). The ZS source at a frequency of 164 MHz drifted southward, i.e., in the direction opposite to the drift of the sources of type III bursts.

Taking into account the above assumption, this indicates that the fast electron beams accelerated in the lower lying current sheet (it is these beams that are responsible for periodic type III bursts) are reflected from the region with a magnetic shear. The loss-cone velocity distribution of the reflected particles leads to the generation of plasma waves and whistlers, whose interaction produces a ZS at corresponding frequencies. The fact that the direction of the spatial drift of the ZS source and the sign of the frequency drift change simultaneously indicates that the spatial drift at a fixed frequency is not an actual shift of the source, but rather a displacement of the energy maximum in the vertical direction within a finite-size plasma region that radiates at this frequency (due to the velocity spread of the fast

particles) and also along a surface of equal density. Within the adopted whistler model, such a drift is quite realistic.

The excitation of whistlers by the reflected particles (which have a loss-cone velocity distribution) should occur at the anomalous Doppler resonance, at which the particles and waves propagate in the same direction. A positive frequency drift of the ZS stripes indicates that, in this case, whistlers propagate downward. Quasilinear scattering of whistlers by fast particles deforms the electron distribution function: the longitudinal velocities decrease, whereas the transverse anisotropy increases. As a result, the excitation of whistlers switches to the normal Doppler resonance, at which the particles and waves propagate in different directions, and whistlers began to propagate upward (see [16] for details). The switching occurs at the instants at which the ZS frequency drift changes its sign and the ZS source begins to drift in the opposite direction. Two such instants are marked in Fig. 2b by light vertical lines.

Even greater shifts of the source center occur at the instants corresponding to the boundaries of the ZS absorption stripes. In this case, an angular shift of ~4.8' over 1/3 s (e.g., within the time interval 10:08:41.3–10:08:41.7 UT), which formally corresponds to velocities exceeding the speed of light, cannot be associated with the actual motion of particles. Such a fast angular shift is actually related to the switching of the source image to the maximum of the emission continuum, which indeed corresponds to an angular shift of more than 4' in the south–west direction above the maximum of the SXR burst (see Fig. 1).

Thus, although the centers of the sources of the ZS and type III bursts almost coincide, the emission is produced by different particles moving in different directions: for type III bursts, these are particle beams propagating from the acceleration region, which is the highest part of the burst current sheet (the height of this region corresponds to $f_{pe} \approx 450$ MHz), whereas for the ZS, these are the particles reflected from the region with a magnetic shear (at the height that corresponds to the minimal frequency of type III bursts and where $f_{pe} \approx$ 125 MHz). A new abrupt perturbation, which partially stops the frequency drift of type III bursts at 10:07:37–10:07:58 UT, indicates the position of a new X-point of magnetic reconnection (at the height where $f_{pe} \approx$ 170 170 MHz). At such heights, the particles generating type III bursts are partially captured in a new magnetic cloud (an island above the X-point). The size of this new magnetic cloud (between the new X-point and the sheared magnetic field) determines the initial ZS frequency range. Over 1 min (from 10:08 to 10:09 UT), whistlers gradually propagate downward to the region where $f_{pe} \approx 210$ MHz.

The large transverse size of the source indicates that whistlers are excited throughout the entire layer with a given plasma density above the AR. However, the maximum of the radio emission intensity can be greatly shifted along this layer from the center of continuum. In the whistler model, each ZS stripe is related to an individual whistler packet. The ZS periodicity is mainly related to the periodicity of the quasilinear interaction of whistlers with fast particles (the periodic deformation of the electron distribution function). The ZS periodicity can also be caused by the periodicity in injection of fast particles and by the bounce motion of particles in a magnetic trap.

In the event under study, there were no explicit evidence of a trap, but an amazing coincidence was observed between the number of type III bursts (24 bursts) within the time interval 10:08–10:09 UT and the number of the ZS stripes along the time axis in the dynamic spectrum. Quasilinear effects lead to an additional modulation along the ZS stripes. These effects come into play only when the particles propagate together with waves (whistlers). A gradual shift of the ZS hump accompanied by the change in the sign of the frequency drift (two such shifts are marked by dark curves in Fig. 2a) is caused by the diffusion of whistlers on fast particles under conditions such that the switching between resonances (see above) at different frequencies (heights) occurs with a small time delay equal to the diffusion time at a given height.

The double plasma resonance model proposed for this event in [25] does not explain the effects observed. First of all, it fails to predict the number of the ZS stripes in the frequency range of interest. If we consider realistic (rather than hypothetical) height profiles of the plasma density and the magnetic field above the AR, e.g., the double Newkirk model ($n = 16.52 \times 10^4 \times 10^{4.32/h}$ cm$^{-3}$, where $h$ is the distance from the center of the Sun in units of the solar radius) and a dipole magnetic field whose height scale is much smaller than the height scale of the plasma density, then, instead of the observed eighteen stripes in the 135- to170-MHz frequency range, we will obtain only ten stripes with harmonic numbers $s$ varying from 10 to 20, as is shown in Fig. 3. Moreover, this model predicts a sharp increase in the frequency separation between the stripes (from 2.5 to 7 MHz), rather than an actually observed gradual increase from 1.7 to 2.2 MHz.

All the other models (e.g., those with the plasma density profile described by the barometric formula and the magnetic field profile considered in [38]) even greater disagree with observations. We note that the magnetic field model proposed in [38] is quite appropriate because it is confirmed by numerous radio observations. On the other hand, the barometric formula certainly does not apply to magnetic loops with $\beta \ll 1$, because this formula describes the density profile in a gravitational field at a constant temperature without allowance for the magnetic field.

Thus, the ZS contains not only the emission stripes but also absorption stripes, which are sometimes dominant. In this context and also taking into account the

simultaneous generation of the ZS, fiber bursts, and fast pulsations, the main properties of the ZS in the event under study can hardly be explained in terms of the new model proposed in [21]. It is quite reasonable to assume that electrostatic plasma waves and whistlers are excited in new burst loops by the trapped fast particles. However, it is not so obvious whether there are necessary conditions (first of all, the condition $T_e \gg T_i$ [22]) for the generation of small-scale inhomogeneities (ion-acoustic solitons); in [21], their presence was merely postulated. There is also a doubt whether the model [21] applies to the meter wavelength range because, in this range, the wavelength is on the order of the inhomogeneity length ($\lambda \sim L$). It should be emphasized that the main condition for the applicability of geometrical optics in deriving the eikonal equations in [21] (see formulas (4) and (5) in that paper) is the inequality $\lambda \ll L$.

## 5. CONCLUSIONS

ZS stripes against the background of type III bursts in the 1994 10 25 event have been considered. The main specific feature of this event is that the fixed-frequency sources of type III radio bursts and the individual ZS stripes drifted in space in opposite directions, whereas their centers coincided in the Nançay interferometer maps. The change in the sign of the frequency drift of the ZS stripes correlated with that of the spatial drift of the radio source at a frequency of 164 MHz. The excitation of the ZS stripes has been analyzed in terms of the interaction of periodic whistler packets with plasma waves. It has been shown that type III bursts and the ZS stripes are excited by different particles moving in opposite directions. In particular, whistlers are excited by the particles reflected from regions with a transverse magnetic field (magnetic reconnection regions in the upper corona). The whistler model accounts for a large number of the ZS stripes, the frequency separation between which gradually increases with frequency (plasma density) in accordance with the double Newkirk model. In contrast to the double plasma resonance model, the model involving quasilinear interaction of whistlers with fast particles allows one to explain all the fine effects of the ZS dynamics.

## ACKNOWLEDGMENTS

I am grateful to M. Poquerusse, K.-L. Klein, and P. Zlobec for providing me with the observational data. This study was supported in part by the Russian Foundation for Basic Research, project no. 02-02-16201.

## REFERENCES

1. C. Slottje, *Atlas of Fine Structures of Dynamical Spectra of Solar Type IV-dm and Some Type II Bursts* (Utrecht Observatory, Utrecht, 1981).
2. A. Kruger, *Introduction to Solar Radio Astronomy and Radio Physics* (Reidel, Dordrecht, 1979; Nauka, Moscow, 1983).
3. G. P. Chernov, L. V. Yasnov, Y. Yan, and Q. Fu, China Astron. Astrophys. **1**, 525 (2001).
4. G. P. Chernov, Y. Yan, and Q. Fu, Astron. Astrophys. **406**, 1071 (2003).
5. J. Kuijpers, Collective Wave–Particle Interactions in Solar Type IV Radio Sources (Utrecht University, Utrecht, 1975).
6. V. V. Zheleznyakov and E. Ya. Zlotnik, Solar Phys. **44**, 461 (1975).
7. V. V. Zheleznyakov, *Electromagnetic Waves in Space Plasma* (Nauka, Moscow, 1977).
8. L. Mollwo, Solar Phys. **83**, 305 (1983).
9. L. Mollwo, Solar Phys. **116**, 323 (1988).
10. R. M. Winglee and G. A. Dulk, Astrophys. J **307**, 808 (1986).
11. O. A. Mal'tseva and G. P. Chernov, Kinemat. Fiz. Nebesnykh Tel **5** (6), 32 (1989).
12. O. A. Mal'tseva and G. P. Chernov, Kinemat. Fiz. Nebesnykh Tel **5** (6), 44 (1989).
13. G. P. Chernov, Solar Phys. **130**, 234 (1990).
14. G. P. Chernov, Astron. Zh. **67**, 126 (1990) [Sov. Astron. **34**, 66 (1990)].
15. G. P. Chernov, A. K. Markeev, M. Poquerusse, *et al.*, Astron. Astrophys. **334**, 314 (1998).
16. G. P. Chernov, Astron. Zh. **73**, 614 (1996) [Astron. Rep. **40**, 561 (1996)].
17. G. P. Chernov, Astron. Zh. **53**, 1027 (1976) [Sov. Astron. **20**, 582 (1976)].
18. G. P. Chernov, Astron. Zh. **66**, 1258 (1989) [Sov. Astron. **33**, 649 (1989)].
19. G. P. Chernov and V. V. Fomichev, Pis'ma Astron. Zh. **15**, 947 (1989) [Sov. Astron. Lett. **15**, 410 (1989)].
20. V. G. Ledenev, M. Karlicky, Y. Yan, and Q. Fu, Solar Phys. **202**, 71 (2001).
21. J. LaBelle, R. A. Treumann, P. H. Yoon, and M. Karlicky, Astrophys. J. **593**, 1195 (2003).
22. S. A. Kaplan and V. N. Tsytovich, *Plasma Astrophysics* (Nauka, Moscow, 1972; Pergamon, Oxford, 1974).
23. H. Aurass, B. Vrsnak, A. Hofmann, and V. Ruzdjak, Solar Phys. **190**, 267 (1999).
24. P. K. Manoharan, L. van Driel-Gesztelyi, M. Pick, and P. Demoulin, Astrophys. J, **468**, L73 (1996).
25. V. V. Zaĭtsev and E. Ya. Zlotnik, in *Proceedings of the Conference on Active Processes in the Sun and Stars, St. Petersburg, 2002* (NIIRF SPbGU, St Petersburg, 2002), p. 257.
26. G. P. Chernov, K.-L. Klein, P. Zlobec, and H. Aurass, Solar Phys. **155**, C. 373 (1994).
27. V. N. Tsytovich, *Nonlinear Effects in Plasmas* (Nauka, Moscow, 1967; Plenum, New York, 1970).
28. V. N. Tsytovich, *Theory of Turbulent Plasma* (Atomizdat, Moscow, 1971; Plenum, New York, 1974).
29. V. V. Fomichev and S. M. Faĭnshteĭn, Astron. Zh. **65**, 1058 (1988) [Sov Astron. **32**, 552 (1988)].
30. E. Jamin, D. Parkinson, A. Rogister, and M. Bernatici, Phys. Fluids **17**, C. 419 (1974).

31. R. Gendrin, Geophys. Space Phys **19**, 171 (1981).

32. P. A. Bespalov and V. Yu. Trakhtengerts, *Alfvén Masers* (IPFAN, Gorki, 1986).

33. P. A. Bespalov and V. Yu. Trakhtengerts, Geom. Aéron. **14**, 321 (1974).

34. B. N. Breĭzman, in *Reviews of Plasma Physics*, Ed. by B. B. Kadomtsev (Énergoatomizdat, Moscow, 1987; Consultants Bureau, New York, 1990), Vol. 15.

35. Y. Omura and M. Matsumoto, J. Geophys. Res. **92**, 8649 (1987).

36. V. D. Shapiro and V. I. Shevchenko, Itogi Nauki Tekhn., Ser: Astronomiya **32**, 235 (1987).

37. V. V. Parail and O. P. Pogutse, in *Reviews of Plasma Physics*, Ed. by M. A. Leontovich and B. B. Kadomtsev (Atomizdat, Moscow, 1982; Consultants Bureau, New York, 1986), Vol. 11.

38. G. A. Dulk and D. J. McLean, Solar Phys. **57**, 279 (1978).

*Translated by N.N. Ustinovskiĭ*

SPELL: 1. nonducted, 2. ducted, 3. unducted, 4. switchings, 5. sawtooth